

# Glancing angle deposition for tuning electronic transport properties of Si thin films

Stefania Oliveri<sup>1</sup>, Jean-Marc Cote<sup>2</sup>, Marina Raschetti<sup>1</sup>, Pierre Roux<sup>3</sup>, Nicolas Martin<sup>2</sup> \*

<sup>1</sup> Université de Franche-Comté, CNRS, Institut FEMTO-ST, F-25000 Besançon, France

<sup>2</sup> SUPMICROTECH, CNRS, Institut FEMTO-ST, F-25000 Besançon, France

<sup>3</sup> Université de Franche-Comté, SUPMICROTECH, CNRS, Institut FEMTO-ST, F-25000 Besançon, France

## Abstract

We report on electronic transport properties of B-doped Si thin films 400 nm thick sputter-deposited by glancing angle deposition (GLAD). For each film, a fixed deposition angle  $\alpha$  is used during the growth. A series of 9 films are prepared changing  $\alpha$  from  $0^\circ$  to  $80^\circ$  with increments of  $10^\circ$ . DC electrical resistivity, charge carrier mobility and concentration are systematically measured in the temperature range from 290 K to 410 K. For deposition angles higher than  $40^\circ$ , a tilted columnar morphology appears and becomes more defined, especially for the most grazing angles. The highest deposition angles also lead to more resistive films with charge carrier mobility and concentration significantly changing for  $\alpha > 30^\circ$ . Experimental results are discussed assuming the evolution of structural defects vs. deposition angle in the columnar architecture of Si GLAD films.

## Keywords

Glancing Angle Deposition, silicon films, electrical resistivity, carrier mobility, carrier concentration.

## 1. Introduction

It is well known that semiconducting behaviors of Si films can be adjusted in useful ways by modifying the structure, the chemical composition or more commonly by introducing impurities with a doping approach [1]. However, doping limitations have induced an important bottleneck in emerging device technologies putting stringent demands on nanoscale control of electronic properties of semiconductor materials [2]. Although fabrication processes based-on a

---

\* Corresponding author: nicolas.martin@femto-st.fr

well-controlled introduction of impurities still remain one of the most efficient strategies to change electronic properties of semiconductors, recent advances focused on nanostructuring of thin films have emerged as an original approach to extend their electronic transport properties [3]. Among these new developments, the GLancing Angle Deposition (GLAD) technique has turned out into an attractive method to produce original surface morphologies, especially for designing innovative architectures [4], but also for tuning the degree of porosity in the as-deposited thin films. Such a tunable porosity induced by the GLAD growth is of primary importance for controlling electronic transport properties in Si thin films [5-7]. If electrical conductivity of GLAD films has commonly been investigated for several metallic films exhibiting tilted columnar structures, very little has been reported about electronic transport characteristics of semiconducting materials, the basic ones being silicon and germanium [8]. It is thus a relevant scientific motivation to show and understand how a simple management of the columnar structure (by adjusting the deposition angle) enables a precise tailoring of many intrinsic properties of semiconductors, assuming a close connection with the nanoscale engineering obtained in GLAD thin films.

In this letter, we report on electronic transport properties of Si films sputter-deposited by the GLAD technique using a systematic increase of the deposition angle  $\alpha$  from 0 to 80°. DC electrical resistivity and carrier characteristics are systematically determined as a function of temperature for the sputter-deposited Si films in order to show how this simple deposition technique involving a tilting incidence of the sputtered atoms can tune the Si films structure. Relationships between some structural features of Si GLAD films and their electronic transport properties are thus investigated.

## **2. Material and Methods**

Si films were deposited on glass substrates by DC magnetron sputtering in a 120 L chamber evacuated at a base pressure below  $10^{-5}$  Pa. A p-type Si target (6 inch diameter, purity 99.9 at. %, B-doped) was DC sputtered in a pure argon atmosphere. No external heating was applied on the grounded substrates during the deposition stage carried out at room temperature. The GLAD technique was developed to produce tilted columnar architectures ( $\alpha = 0$  to 80°) by means of an increasing deposition angle of 10° with a target-to-substrate distance maintained at 100 mm. The argon mass flow rate was set to 30 sccm and the pumping speed was maintained at 220 L s<sup>-1</sup>. Such operating conditions led to a constant total sputtering pressure of 0.23 Pa. A constant target current of 300 mA was used for all depositions

(sputtering power and target potential of 137 W and 446 V, respectively). The deposition time was adjusted to get a constant film thickness of 400 nm. DC electrical resistivity measurements of Si films deposited on glass substrate were performed in air with a temperature ranging from 290 to 410 K using the van der Pauw configuration (4 probe method). Carrier mobility and carrier concentration were similarly determined by the Hall effect using the same setup and applying a magnetic field of 0.8 T perpendicular to the sample surface.

### 3. Results and Discussion

DC electrical resistivity of Si GLAD films measured at room temperature remains nearly unchanged around  $\rho_{298K} = 4.1\text{-}4.6 \text{ } \Omega \text{ m}$  for deposition angles  $\alpha$  lower than  $40^\circ$  (Fig. 1). These resistivity values are higher than that of polycrystalline Si material ( $\rho_{300K} = 4.2 \times 10^{-2} \text{ } \Omega \text{ m}$  for undoped-Si [9]) since sputter-deposited thin films by GLAD typically exhibit a poorly crystalline or even an amorphous structure with voids and defects in the columnar structure (to see Fig. S1 in Supplementary Material). For this range of deposition angles, the shadowing effect induced by the GLAD process is not efficient enough to modify the overall films microstructure (no clear features or tilted columns can be observed on the SEM top and cross-section views as shown in Fig. S2 in Supplementary Material). However, carrier concentration as well as mobility both exhibit a reverse evolution vs. deposition angle with a peculiar value at  $\alpha = 30^\circ$  (minimum of carrier mobility and maximum of carrier concentration leading to a nearly invariant resistivity). These optimal values cannot be assigned to changes of grain size since all films are amorphous. It is rather connected to stress variation commonly reported for metallic [10] and ceramic [11, 12] GLAD films for deposition angles close to  $30^\circ$ . A stress relaxation is typically reported when the deposition angle is higher than  $30^\circ$ . As the deposition angle increases, shadowing effect becomes significant leading to a more voided structure and developing structural defects. As result, a stress reduction in Si films occurs, which induces enhancement of the carrier mobility due to variation of the effective mass of free carriers [13]. A further increase of the deposition angle lowers the carrier concentration and favors the mobility. The latter reaches  $\mu_{298K} = 4.39 \times 10^{-1} \text{ m}^2 \text{ V}^{-1} \text{ s}^{-1}$  for  $\alpha = 80^\circ$  whereas the carrier concentration reduces down to  $p_{298K} = 1.99 \times 10^{18} \text{ m}^{-3}$ . Similarly, electrical resistivity abruptly rises from  $\alpha = 50^\circ$  and overpasses  $1.35 \times 10^1 \text{ } \Omega \text{ m}$  for  $\alpha = 80^\circ$ . This behavior is directly connected to some disorders of the film microstructure (especially porosity) produced by the shadowing effect during the columnar growth. It is worth noting that SEM pictures (to see Supplementary Material) do not exhibit some clear nanorods, as sometimes observed in other types of GLAD films

[12, 14]. This is mainly assigned to our deposition conditions, which produce a poorly directive flux of Si atoms (a part is certainly thermalized due to the high substrate-to-target distance used in this study, i.e., 10 cm, and the sputtering pressure of 0.23, which cannot be reduced even more without jeopardizing the plasma stability). As a result, the growth of clear and well-separated nanocolumns is in some extent unfavored. They become relevant for deposition angles  $\alpha$  higher than  $50^\circ$  as commonly observed for many sputter-deposited materials [4] and often reported as critical angles giving rise to significant modifications of many physical properties of GLAD films [14]. Similarly, the amount of growing defects increases as  $\alpha$  rises, which favors the trapping phenomena of carriers and reduces their concentration. This range of deposition angles ( $30$  to  $50^\circ$ ) corresponds to an enhancement of the geometric shadowing effect during the growth. The latter becomes more and more significant as the deposition angle overpasses such a range, giving rise to strong changes of the film properties. Electrical resistivity is particularly affected by grazing deposition angles producing structural defects and developing a voided structure at micro- and nanoscales, which both disturb characteristics of the free carriers.

For all Si GLAD films, the resistivity exhibits an expected temperature dependence corresponding to a semiconducting-like behavior, but with a strong influence of the deposition angle (Fig. 2). Assuming a typical Arrhenius equation (exponential law of electrical conductivity vs. temperature), the activation energy  $E_a$  calculated for each deposition angle remains again nearly constant in-between 129-147 meV up to  $\alpha = 50^\circ$ . Increasing the deposition angle leads to a gradual drop of  $E_a$ , the latter reaching 90 meV for the highest angles. This ease of thermally activated electrical conduction in GLAD Si films prepared with the most glancing angles is related to structural defects induced by the oblique angle deposition process, and also impurities such as oxygen incorporated in the porous structure intrinsic to the tilted columnar architecture. It has been previously reported that defects [15] as well as oxygen atoms [16] in Si material both reduce the energy gap. Since the GLAD process particularly produces growing defects and a porous columnar structure at high deposition angles ( $\alpha > 70^\circ$ ), they contribute to decrease the activation energy.

The effect of deposition angle on electronic transport properties of Si GLAD films is also well illustrated by plotting carrier mobility vs. carrier concentration (Fig. 3). A typical decrease of mobility can be observed when concentration rises as commonly stated for silicon or other semiconducting compounds. This trends also correlates with structural changes of the GLAD Si films when tuning the deposition angle. The shift to lower carrier concentrations and higher

mobilities as  $\alpha$  rises corresponds to semiconducting compounds containing a high amount of growing defects (stacking faults and point defects). It is worth noting that as the temperature increases, the slope given by the log-log mobility *vs.* concentration plot tends to reduce as the deposition angle rises (particularly significant from  $\alpha > 50^\circ$ , and even more visible for  $\alpha = 80^\circ$  in Fig. 3). This support again the growing influence of scattering by defects on carrier mobility as the deposition angle tends to grazing values ( $\alpha > 70^\circ$ ). The mobility model proposed by Caughey and Thomas [17] can be used as a basic equation for fitting experimental data (calculated only at 290 K for clarity). A typical sigmoidal curve is obtained optimizing the fitting parameters, i.e., low  $\mu_{min}$  and high  $\mu_{Max}$  carrier mobilities, reference carrier concentration  $p_{Ref}$  and slope of the fit  $a$  (inset in Fig. 3). It shows again that an increase of the deposition angle favors structural defects in the Si columnar structure. Since the carrier lifetime is dominated by the recombination process through shallow states produced by intra-grain defects, the carrier concentration is reduced for high deposition angles. With an increase of temperature from 290 to 410 K and for any deposition angle, the formation of free carriers in the conduction band prevails over the recombination process. Similarly, scattering of carriers by lattice vibrations is favored as the temperature rises leading to a lower carrier mobility.

#### 4. Conclusion

Electronic transport properties of Si thin films 400 nm thick sputter-deposited by the GLAD technique were investigated. The deposition angle  $\alpha$  was gradually changed from  $0^\circ$  to  $80^\circ$ . DC electrical resistivity at room temperature was unchanged and in-between 4.1-4.6  $\Omega$  m for films prepared with the lowest angles ( $\alpha < 50^\circ$ ). A further increase of  $\alpha$  gave rise to an abrupt increase of resistivity with  $\rho_{298K} = 1.35 \times 10^1 \Omega$  m as the deposition angle was set to  $80^\circ$ . This range of angles was correlated with significant microstructural modifications of the films induced by the shadowing effect becoming the key parameter at grazing deposition angles. On the other hand, carrier mobility and concentration exhibited a reverse evolution *vs.* deposition angle with a peculiar value at  $\alpha = 30^\circ$  (corresponding to a nearly constant resistivity). It was argued that growing defects (especially stacking faults and point defects) increased as a function of the deposition angle  $\alpha$ , favoring the trapping phenomena of free carriers reducing their concentration and enhancing their mobility when  $\alpha$  reached the most grazing angles ( $\alpha > 70^\circ$ ). Mobility *vs.* concentration of the free carriers showed a typical sigmoidal Caughey-Thomas curve with a reduced concentration and improved mobility

for the highest deposition angles. This evolution was again related to the structural defects in the Si columnar architecture induced by the GLAD growth.

### **CRedit authorship contribution statement**

Stefania Oliveri: Writing - Data curation. Jean-Marc Cote: Data curation. Marina Raschetti: Data curation. Pierre Roux: Review & editing. Nicolas Martin: Writing - Review & editing.

### **Declaration of Competing Interest**

The authors declare that they have no known competing financial interests or personal relationships that could have appeared to influence the work reported in this paper.

### **Acknowledgements**

This work was supported by the EIPHI Graduate School (contract ANR-17-EURE-0002), the Region of Bourgogne Franche-Comté and the French RENATECH network.

### **Appendix A. Supplementary material**

Supplementary material related to this article can be found online at <https://...>

### **Data availability**

Data will be made available on request.

### **References**

- [1] O. Astakhov, R. Carius, F. Finger, Y. Petrusenko, V. Borysenko, D. Barankov, Relationship between defect density and charge carrier transport in amorphous and microcrystalline silicon, *Phys. Rev. B*, 79 (2009) 104205-14. <https://doi.org/10.1103/physrevb.79.104205>
- [2] W. Walukiewicz, Intrinsic limitations to the doping level of wide-gap semiconductors, *Physica B*, 302-303 (2001) 123-134. [https://doi.org/10.1016/s0921-4526\(01\)00417-3](https://doi.org/10.1016/s0921-4526(01)00417-3)

- [3] S. Zhang, Nanostructured thin films and coatings, CRC Press, Boca Raton, (2010).  
<https://doi.org/10.1201/9780429150999>
- [4] M.M. Hawkeye, M.T. Taschuk, M.J. Brett. Glancing Angle Deposition of Thin Films, John Wiley & Sons Ltd, Chichester (2014). <https://doi.org/10.1002/9781118847510>
- [5] P. Sharma, X. Sun, G. Parish, A. Keating, Optimising porous silicon electrical properties for thermal sensing applications, Microporous Mesoporous Mater., 312 (2021) 110767-9.  
<https://doi.org/10.1016/j.micromeso.2020.110767>
- [6] X. Sun, P. Sharma, G. Parish, A. Keating, Enabling high-porosity silicon as an electronic material, Microporous Mesoporous Mater., 312 (2021) 110808-10. <https://doi.org/10.1016/j.micromeso.2020.110808>
- [7] B. Terheiden, J. Hensen, A. Wolf, R. Horbelt, H. Plagwitz, R. Brendel, Layer Transfer from Chemically Etched 150 mm Porous Si Substrates, Materials, 4 (2011) 941-952. <https://doi.org/10.3390/ma4050941>
- [8] H.G. Chew, W.K. Choi, W.K. Chim, E.A. Fitzgerald, Fabrication of germanium nanowires by oblique angle deposition, Int. J. Nanosci., 5 (2006) 523-527. <https://doi.org/10.1142/s0219581x06004735>
- [9] E. Munoz, J.M. Boix, J. Llabres, J.P. Monico, J. Piqueras, Electronic properties of undoped polycrystalline silicon, Solid State Electron., 17 (1974) 439-446. [https://doi.org/10.1016/0038-1101\(74\)90073-2](https://doi.org/10.1016/0038-1101(74)90073-2)
- [10] H.Z. Yu, C.V. Thompson, Effects of oblique-angle deposition on intrinsic stress evolution during polycrystalline film growth, Acta Mater., 77 (2014) 284-293. <https://doi.org/10.1016/j.actamat.2014.05.060>
- [11] F. Grigoriev, V.B. Sulimov, A.V. Tikhonravov, Atomistic simulation of stresses in growing silicon dioxide films, Coatings, 10 (2020) 220-10. <https://doi.org/10.3390/coatings10030220>
- [12] G. Abadias, F. Angay, R. Mareus, C. Mastail, Texture and stress evolution in HfN films sputter-deposited at oblique angles, Coatings, 9 (2019) 712-15. <https://doi.org/10.3390/coatings9110712>
- [13] S. Dhar, E. Ungersbock, H. Kosina, T. Grassler, S. Selberherr, Electron mobility model for <110> stressed silicon including strain-dependent mass, IEEE Trans. Nanotechnol., 6 (2007) 97-100.  
<https://doi.org/10.1109/tnano.2006.888533>
- [14] A. Siad, A. Besnard, C. Nouveau, P. Jacquet, Critical angles in DC magnetron glancing thin films, Vacuum, 131 (2016) 305-311. <https://doi.org/10.1016/j.vacuum.2016.07.012>

- [15] P.H. Huang, C.M. Lu, Effects of vacancy cluster defects on electrical and thermodynamic properties of silicon crystals, *Sci. World J.*, (2014) 1-8. <https://doi.org/10.1155/2014/863404>
- [16] A.A. Gnidenko, V.G. Zavodinsky, Effect of oxygen on structure and electronic properties of silicon nanoclusters  $\text{Si}_n$  ( $n = 5, 6, 10, 18$ ), *Semiconductors*, 42 (2008) 800-804. <https://doi.org/10.1134/s1063782608070099>
- [17] D.M. Caughey, R.E. Thomas, Carrier mobilities in silicon empirically related to doping and field, *Proc. IEEE*, 55 (1967) 2192-2193. <https://doi.org/10.1109/proc.1967.6123>

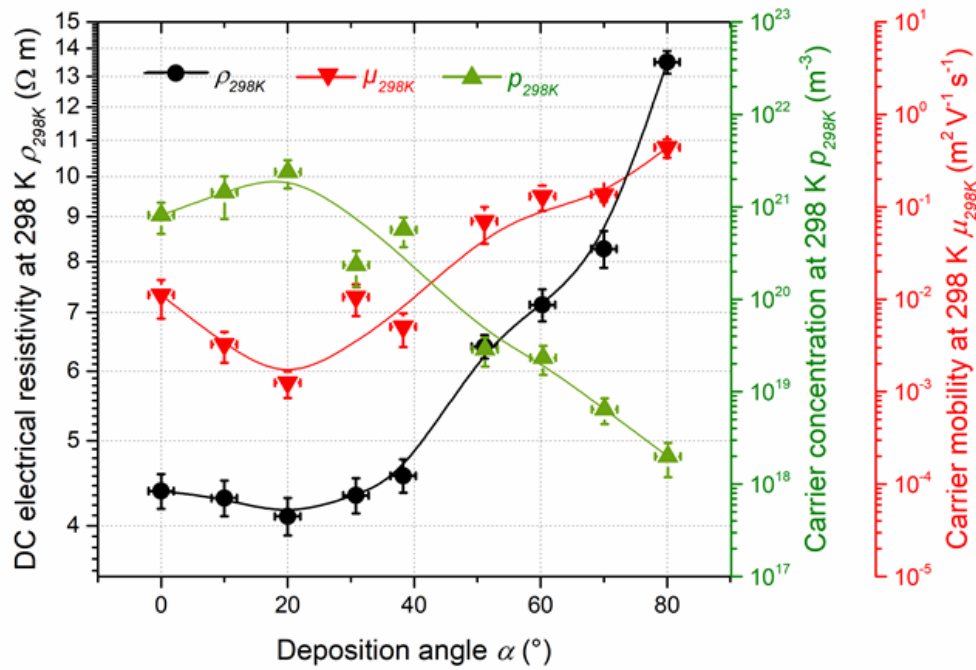


Fig. 1. DC electrical resistivity  $\rho_{298K}$ , carrier concentration  $p_{298K}$  and carrier mobility  $\mu_{298K}$  at room temperature as a function of the deposition angle  $\alpha$  of Si GLAD films 400 nm thick sputter-deposited on glass substrate. Lines are guide for the eye.



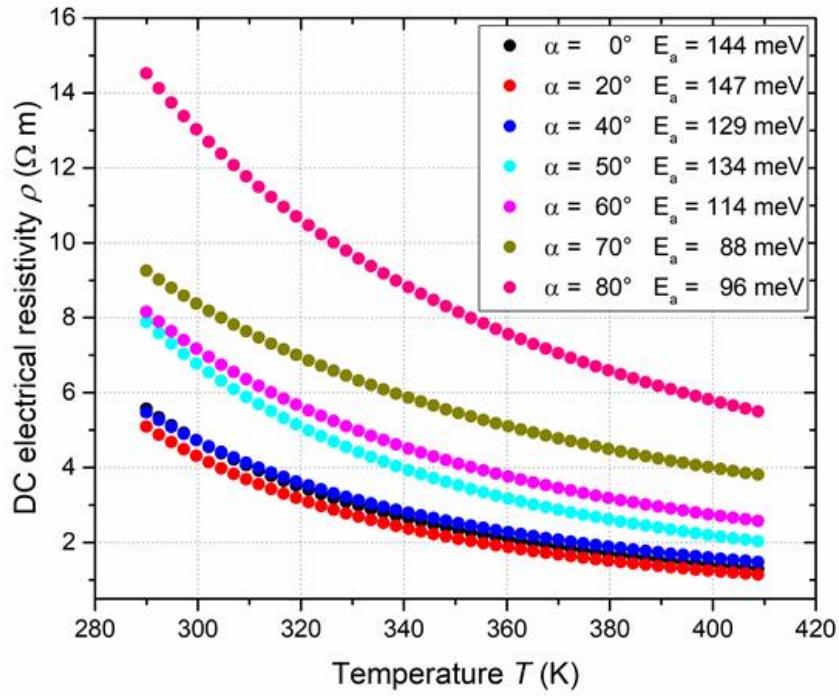


Fig. 2. DC electrical resistivity  $\rho$  vs. temperature  $T$  of Si GLAD films within the temperature range 290-410 K. The deposition angle  $\alpha$  is systematically changed from 0 to 80°. Activation energy is calculated assuming an Arrhenius equation of the electrical conductivity as a function of the temperature.

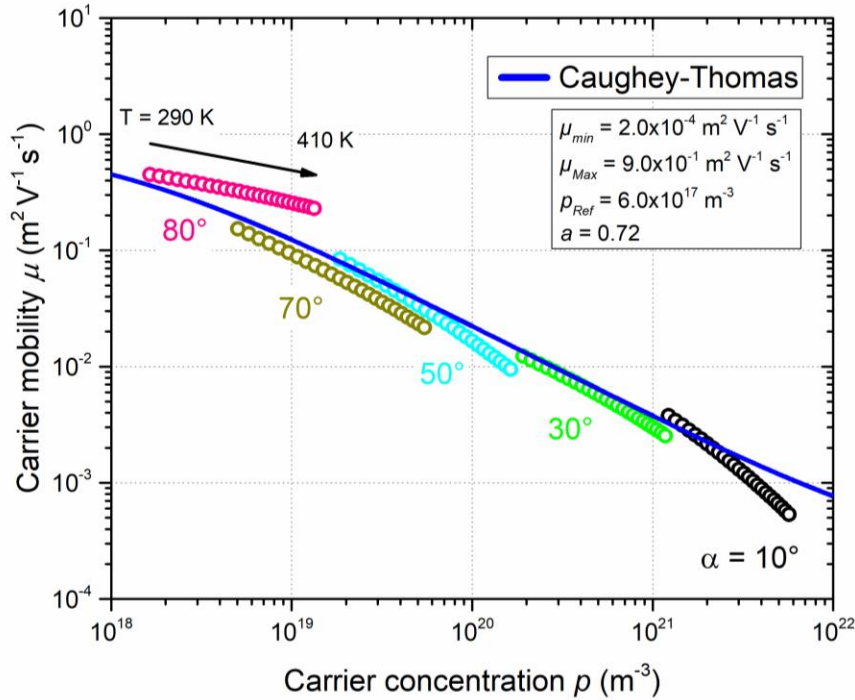


Fig. 3. Carrier mobility  $\mu$  as a function of the carrier concentration  $p$  measured by Hall effect from 290 K to 410 K of Si GLAD films 400 nm thick prepared on glass substrate for different deposition angles  $\alpha$ . The blue line represents the  $\mu$  vs.  $p$  evolution calculated from the fitting parameters optimized at 290 K from the Caughey-Thomas equation [17].  $p_{Ref}$  is the reference carrier concentration,  $a$  is the slope of the fit,  $\mu_{min}$  and  $\mu_{Max}$  are the minimum and maximum mobilities, respectively.

## Supplementary Material

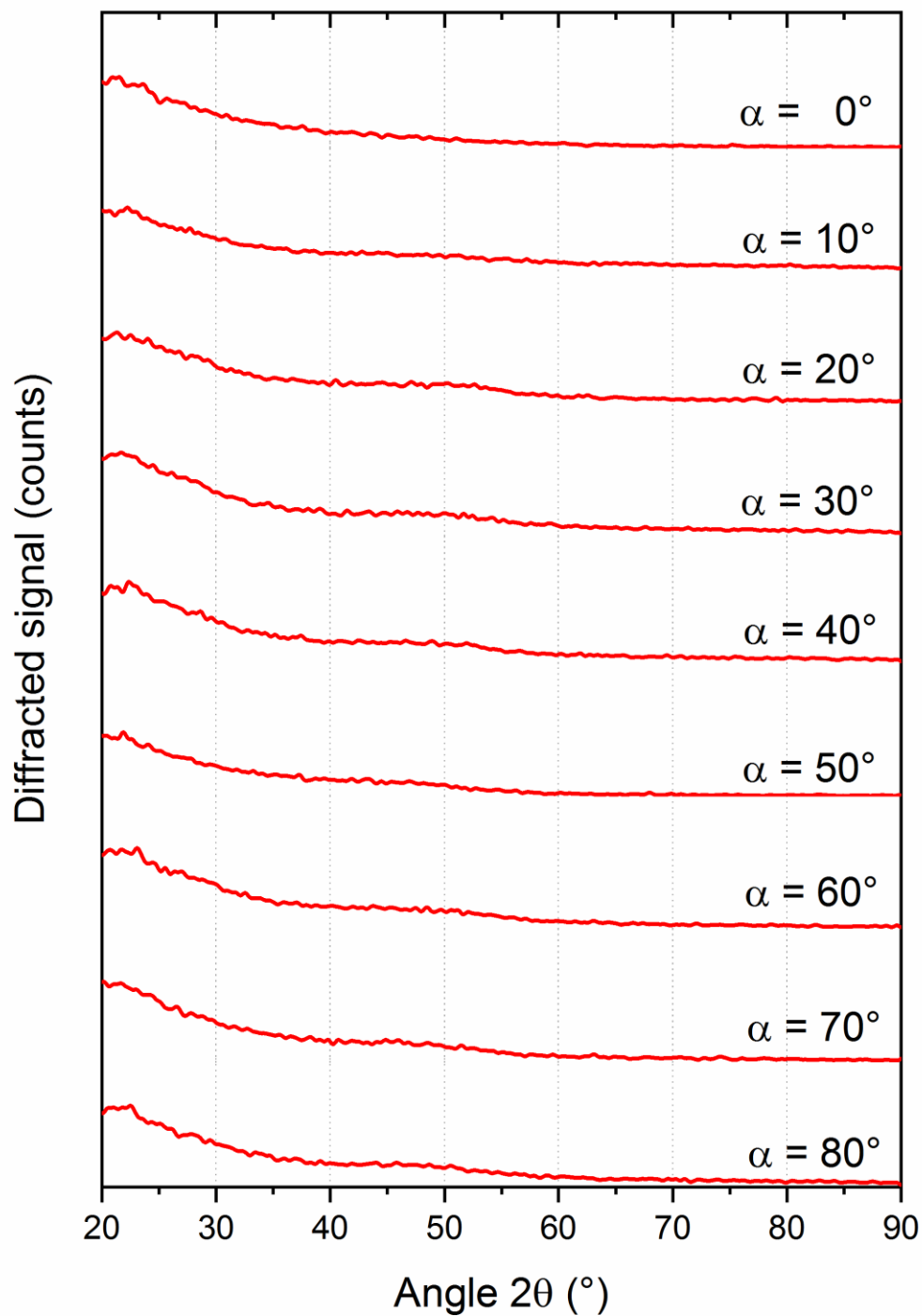


Fig. S1. Grazing-Incidence X-ray Diffraction (GIXRD) patterns measured with an incidence angle  $\theta = 0.8^\circ$  and a scanning range  $2\theta = 20\text{-}90^\circ$  of Si GLAD thin films sputter-deposited on glass with different deposition angles  $\alpha$  from 0 to  $80^\circ$ .

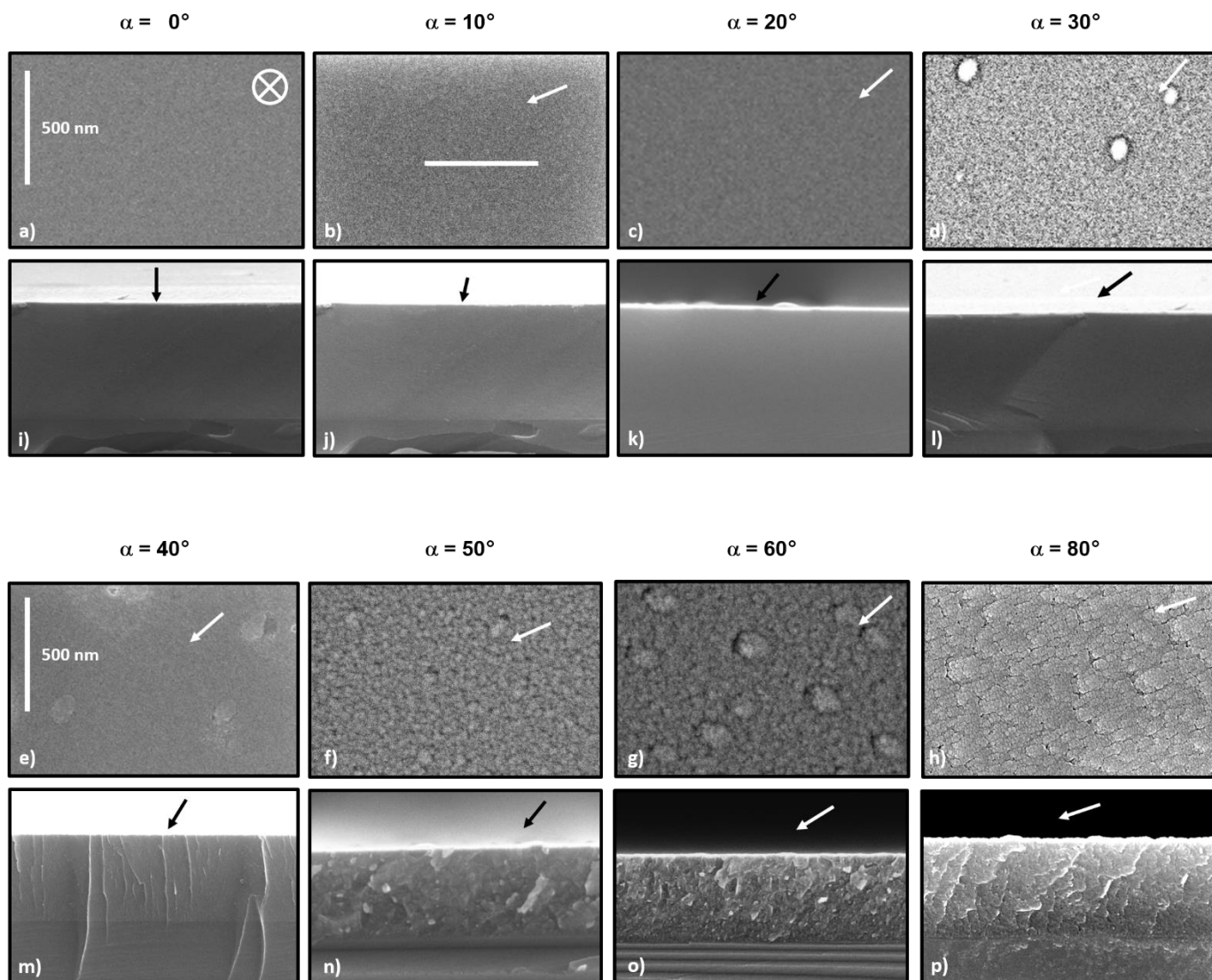


Fig. S2. a) to h) Top and i) to p) cross-section views by Scanning Electron Microscopy (SEM) of Si GLAD thin films prepared with different deposition angles: a), i)  $\alpha = 0^\circ$ ; b), j)  $\alpha = 10^\circ$ ; c), k)  $\alpha = 20^\circ$ ; d), l)  $\alpha = 30^\circ$ ; e), m)  $\alpha = 40^\circ$ ; f), n)  $\alpha = 50^\circ$ ; g), o)  $\alpha = 60^\circ$ ; h), p)  $\alpha = 80^\circ$ ;. Arrows indicate the direction of incoming Si particle flux.

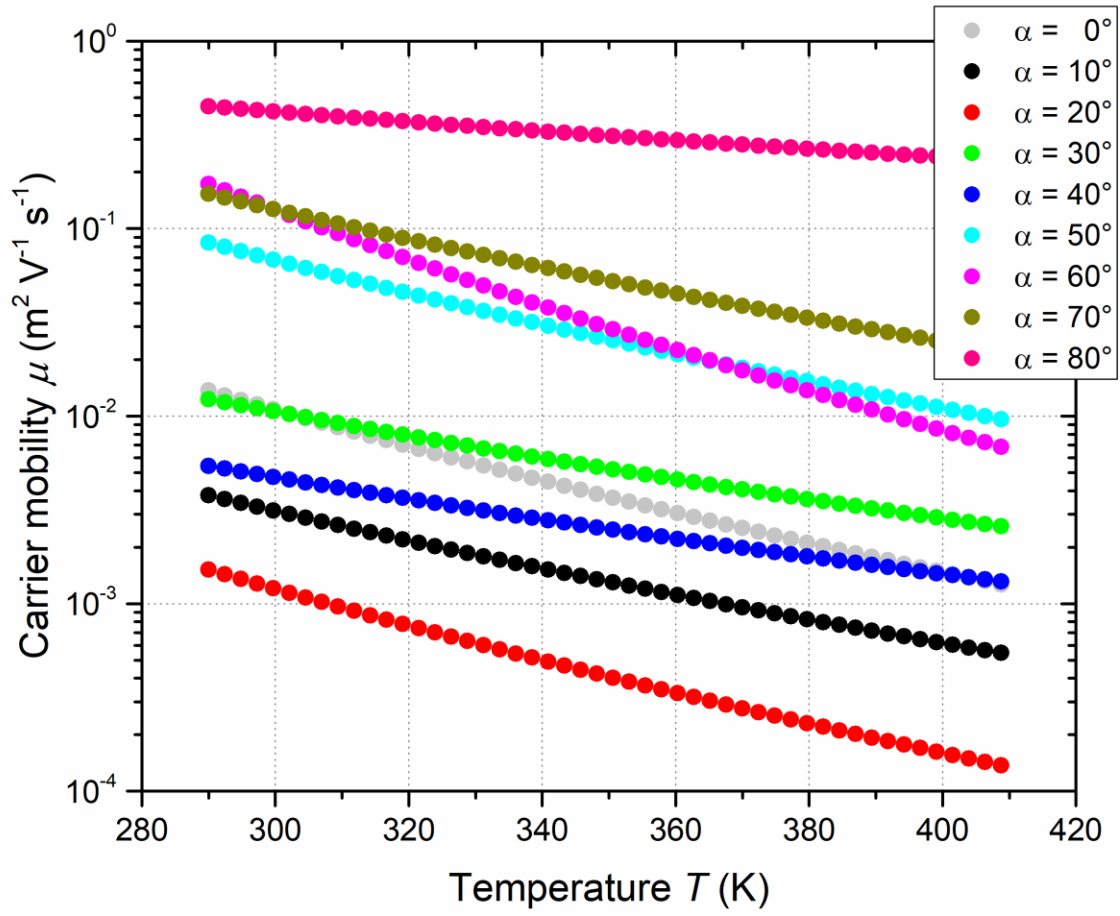


Fig. S3. Carrier mobility  $\mu$  vs. temperature  $T$  measured by Hall effect from 290 K to 410 K of Si GLAD thin films sputter-deposited on glass with different deposition angles  $\alpha$  from 0 to  $80^\circ$ .

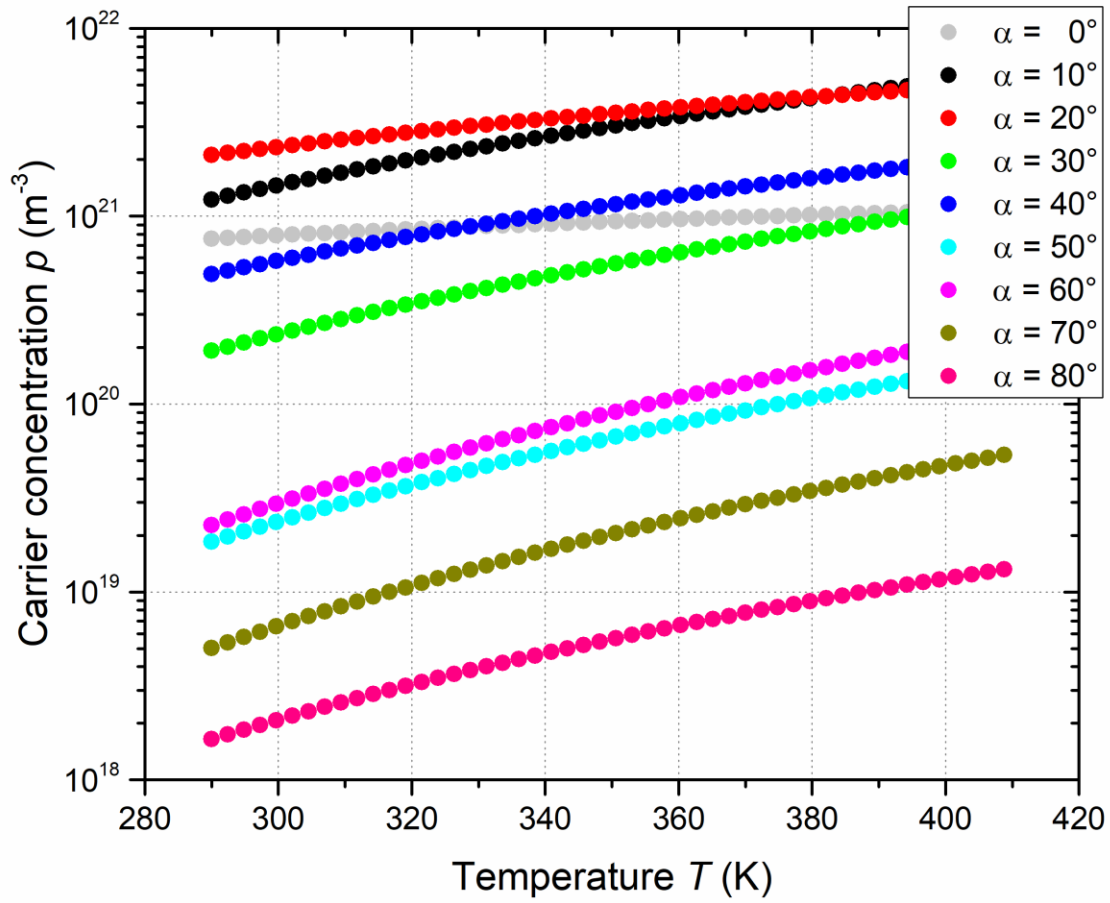


Fig. S4. Carrier concentration  $p$  vs. temperature  $T$  measured by Hall effect from 290 K to 410 K of Si GLAD thin films sputter-deposited on glass with different deposition angles  $\alpha$  from 0 to 80°.